Open Loop Adaptive Coding and Modulation for Mobile Satellite Return Links

Jesús Arnau and Carlos Mosquera
Signal Theory and Communications Department, University of Vigo - 36310 Vigo, Spain.

Abstract

In this work we have tested the applicability of open-loop Adaptive Coding and Modulation (ACM) in the return link of a BGAN-like mobile satellite link using, for improved performance monitoring, effective SNR metrics instead of conventional average SINR as Channel State Information (CSI). After testing the applicability of open-loop CSI, we carried out a performance test focusing on specific working conditions. Results will show that, for the scenario under study, the best performance is obtained in an ITS environment, reaching an improvement of up to 92 % in terms of ASE, and 12 % more availability.

NOMENCLATURE

ACK	Acknowledgement	ACM	Adaptive Coding and Modulation
ASE	Average Spectral Efficiency	ASNR	Average Signal to Noise Ratio
AWGN	Additive White Gaussian Noise	BER	Bit Error Rate
CDF	Cummulative Distribution Function	CSI	Channel State Information
DAMA	Demand Assigned Multiple Acccess	FEC	Forward Error Correction
FL	Forward Link	GEO	Geostationary Orbit
HPA	High Power Amplifier	ITS	Intermediate Tree Shadowed
LMS	Land-Mobile Satellite	LOS	Line-of-Sight
MCS	Modulation and Coding Scheme	MSS	Mobile Satellite System
PDF	Probability Density Function	PHY	Physical (Layer)
QPSK	Quadrature Phase Shift Keying	RL	Return Link
RMS	Root Mean Square	RTT	Round-Trip Time
SIR	Signal-to-Interference Ratio	SINR	Signal-to-Interference-Plus-Noise Ratio
SNR	Signal-to-Noise Ratio		

I. INTRODUCTION

In mobile satellite communications, there is an increasing need for more efficient transmission techniques that enable higher bit-rates at an affordable cost, driven by the increasing consumer needs and the limited spectrum available for mobile satellite systems (MSS). To this extent, Adaptive Coding and Modulation (ACM) allows the provision of broadband services to large user populations at lower costs, since it makes it possible to operate the links more efficiently by selecting the most suitable Modulation and Coding Scheme (MCS) at each time [1].

However, the use of ACM for mobile links operating at L- or S-band is hindered by the long delays in GEO satellites (where the round trip time RTT equals $0.5\,\mathrm{s}$) and the behavior of the Land Mobile Satellite Channel (LMS)[2]. This channel is usually modeled by a fast fading component –whose spectrum is related to the mobile speed by the Doppler effect– superimposed on a slow shadowing component; the parameters of both fading and shadowing depend on the environment in which the receiver happens to be. In short, the mobility of the user terminal will cause fast, difficult to predict channel variations, which will pose additional difficulties on the design of both forward and return link strategies.

As a consequence, new adaptive transmission techniques, as well as statistical modeling tools and simulation approaches are needed to fully exploit the theoretical performance of the channel. In this work, and building on the results from a previous study[3], we developed and tested new adaptation tools for the **return link** targeted at mitigating two of the main problems stated above: the fact that CSI is often stale because of the long delays involved, and the fact that predicting the performance of such a time varying channel is a compelling task even with timely CSI.

To cope with the first problem, our solution is based on **open-loop** adaptation, instead of the conventional closed-loop adaptation; Figure 1 summarizes the differences between the two alternatives: while closed-loop techniques exploit the feedback from the other communication end (delay $\approx$ RTT), open-loop alternatives directly perform measurements on the incoming signal and adapt the transmission parameters accordingly (delay $\approx$ codeword duration). As a consequence, open-loop enjoys information which is up-to-date but may be *partial*: if both links operate on different frequencies their channels will be partially uncorrelated. Also, the co-channel interference levels will be different: interference in the forward link, which is due to the side lobes of the antenna radiation pattern, will be almost constant over time, while in the return link it is related not only to this but also to the number and position of the users transmitting towards the satellite.

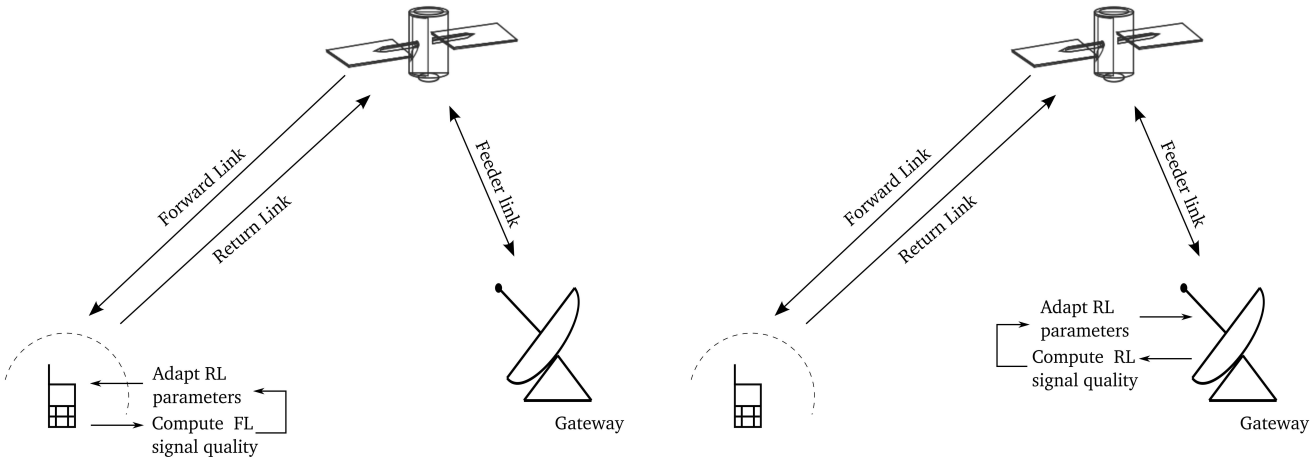

Figure 1. Open-loop (left) against closed-loop (right) adaptation.

Differently from previous works[3], here we focus on BGAN-like systems[4] and test the derived solutions against common impairments found in these kind of systems.

Regarding the mapping of the channel behavior into performance, the usual solution is to average the estimated SINR over a time window (of $0.96\,\mathrm{s}$ in the case of BGAN) and use the resulting value as CSI. Here, and because the same average SINR can be found in quite different channels, we exploited **effective SINR metrics**, borrowed from the physical layer abstraction literature.

The remainder of the document is structured as follows: Section II describes the system and signal model, offering also some information about physical layer abstraction; Section III studies the properties of open-loop CSI; Section IV illustrates the potential of open-loop techniques in terms of availability and spectral efficiency; finally, Section V summarizes the conclusions of the work and proposes two lines of future work.

II. System model

We focus on the return link (RL) of a BGAN-like [4] mobile satellite link operating at L-band; forward and return links are allocated to different frequencies ($1550\,\mathrm{MHz}$ for the forward link and $1650\,\mathrm{MHz}$ for the return link). We assume the existence of pilots, scattered through the payload, that allow accurate channel estimation. The remainder of the section describes the signal model and offers a brief explanation of physical layer abstraction.

A. Signal model

The signal model is given by

$$y_k = \sqrt{\mathrm{snr}} \cdot h_k s_k + w_k \tag{1}$$

with y_k the symbol received at the k-th time instant, s_k the transmitted symbol, h_k the channel coefficient and snr representing the transmitted over noise power; accordingly, w_k comprises the interference and *unit-power noise contribution*.

Next, we offer some more details on these variables.

1) Channel model: We assume h_k follows the 3-state Fontán model [2] for an LMS channel, in which line-of-sight (LOS), small, and heavy shadowing conditions are taken into account by three different *states* following a first-order Markov chain. The parameters of the three states depend on the *environment* in which the terminal is; in other words, the LOS state will exhibit a different behavior depending on whether the terminal is traveling through a desert, a city or a forest, for example.

Focusing on a specific state, the channel behavior follows the Loo model [5]: slow variations in the LOS component (*shadowing*) are described by a log-normal distribution, whereas fast fluctuations of the signal amplitude (*fading*) are given by a Rician distribution.

Mathematically speaking, the probability density function (PDF) of the signal amplitude at a given time instant would be given by

$$f_r(x) = \frac{x}{b_0\sqrt{2\pi d_0}} \int_0^\infty \frac{1}{z} \exp\left(-\frac{(\log z - \mu)^2}{2d_0} - \frac{x^2+z^2}{2b_0}\right) I_0\left(\frac{x\cdot z}{b_0}\right)\, \mathrm{d}z \tag{2}$$

where d_0 is the scale parameter of the log-normal distribution and μ stands for the location parameter of the log-normal distribution.

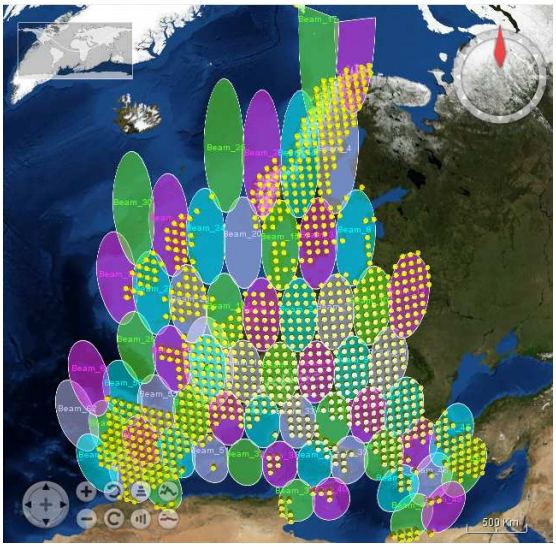

Figure 2. Simulated coverage over Europe.

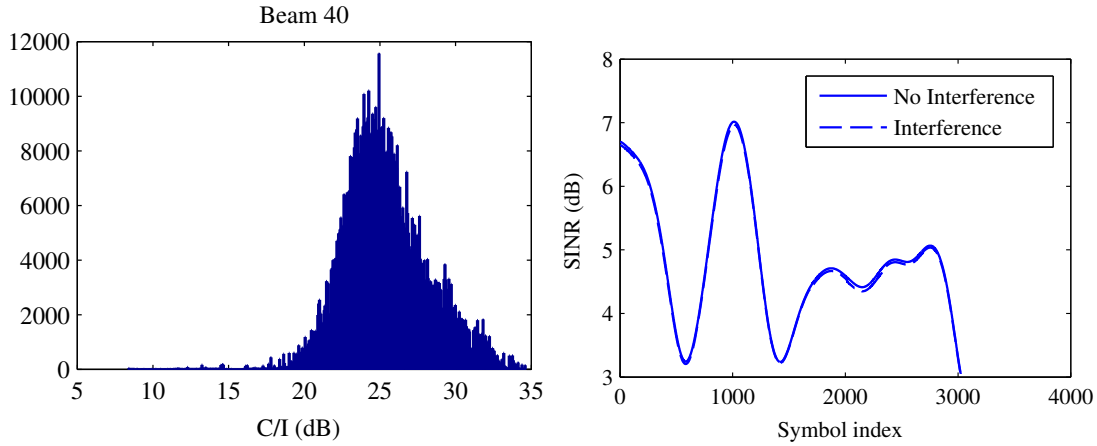

Figure 3. Mild interference profile, named **SI40**. Left is a histogram of the simulated C/I, and right an example of the SINR evolution in an LMS channel including this profile.

From an implementation point of view, the LOS component is obtained by generating independent Gaussian samples n, interpolating them to obtain the correlation properties specified by the model, and then taking $10^{(n/20)}$ to obtain log-normally distributed numbers. The NLOS component, on the other hand, is obtained by filtering Gaussian samples with a low-pass filter; for simplicity, we used a Butterworth filter with 3 dB bandwidth given by the Doppler spread [6], [7].

2) Interference and noise: The sample w_k comprises the effect of noise and interference, so that we can write

$$w_k = n_k + i_k \tag{3}$$

where n_k is a unit-power noise sample (we are already accounting for the noise power in $\sqrt{\text{snr}}$) and i_k is the interference sample.

After simulating a 4-colors, 62-beam coverage over Europe (see Figure 2) in STYLIST[8] (a software tool developed in the framework of an ARTES 5.1 project), we obtained two return link interference profiles, as shown on Figure 3 and Figure 4; these profiles were later on used for the simulations testing the designed ACM techniques.

B. Physical layer abstraction

Obtaining CSI in an LMS channel is a compelling task, among other reasons because it is difficult to capture the channel's behavior with a single parameter. As an example, think of how the average SINR would perform in such an environment, with both LOS and NLOS components possibly changing within the time span of a codeword: the same average SINR value would

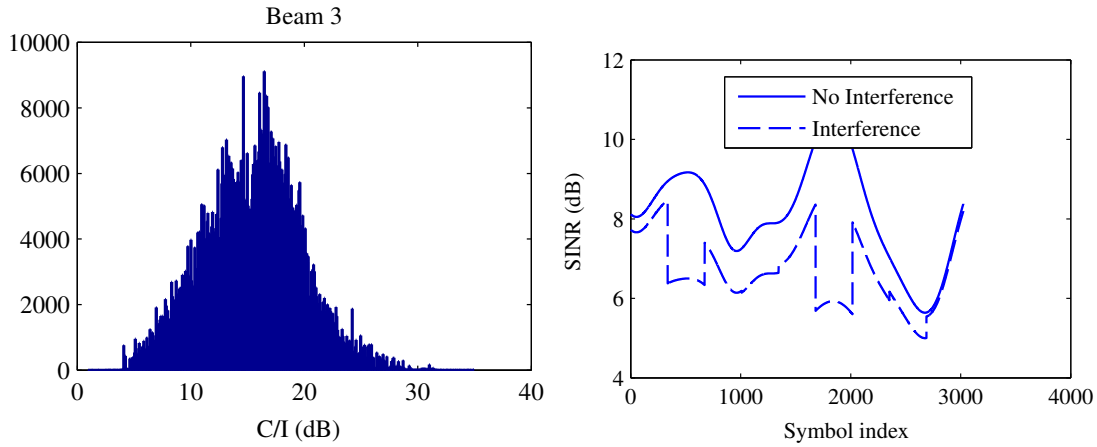

Figure 4. Strong interference profile, named **SI3**. Left is a histogram of the simulated C/I, and right an example of the SINR evolution in an LMS channel including this profile.

appear for very different channel realizations, with different end-to-end performance also. Here, and as in previous works[3], we will use an Effective SNR Mapping (ESM) to tell whether a codeword has been successfully decoded or not. The ESM metric in which we will focus is the Mutual Information Effective SNR Mapping (MIESM), which must be parametrized in terms of just the constellation used, not the code. It reads as

$$\gamma_{eff} = \mathrm{SI}^{-1}\left(\frac{1}{MN}\sum_{n=1}^{N}\mathrm{SI}\left(\gamma_n\right)\right) \tag{4}$$

where M is the number of points in the constellation; if M changes between different symbols, then the normalization term $1/M$ must be included into the summation. SI represents the mutual information associated to a symbol from a constellation with M elements, and is given by [9]:

$$\mathrm{SI} = \log_2 M - \frac{1}{M}\sum_{j=1}^{M}\mathbb{E}_w\left[\log_2\left(1+\sum_{\substack{k=1\\k\neq j}}^{M} e^{-\frac{|x_j-x_k+w|^2-|w|^2}{\sigma^2}}\right)\right]. \tag{5}$$

Here, x_j represents a point in the constellation and w is a zero-mean complex Gaussian random variable with variance $\sigma^2 = 1/(\gamma_n)$. This expression can be easily computed offline for an interval of instantaneous SINRs, where the expected value would be obtained via Monte Carlo: this is the approach we followed in this work. If a closed-form expression is required to perform further analytical studies, then it is possible to approximate SI by a sigmoid function, as explained in [10].

III. Suitability of open-loop CSI

As we said, the channels experienced by FL and RL will be partially uncorrelated. The common assumption is that *the LOS component is still the same, while the NLOS will be completely uncorrelated* (but with the same statistical parameters whenever the frequency separation is not very high). Therefore, before designing an ACM strategy that relies on open-loop CSI, we will need to test how accurate it is, taking into account this partial uncorrelation among the channels.

However, we will show that forward-return uncorrelation is not the only source of impairments: the channel decorrelates after some time –which depends on terminal's speed–, and we need to make use of the obtained CSI before it runs completely stale.

To test the suitability of open-loop CSI, we performed simulations aimed at assessing the impact of the two impairments mentioned above. In this section, we describe the procedure we followed, and report the results obtained.

A. BGAN RL timing

After measuring the signal from the FL, we intend to use it for adapting the RL parameters as soon as possible; the more we wait, the less useful the CSI will be. Unfortunately, compliance with the BGAN standard will enforce a minimum waiting time, approximately given by $n \cdot 80 + \mathrm{SID}$ ms after reception of the first symbol from the FL, where n equals 1 when interleaving is done every 10 ms or 20 ms and n equals 2 when it is done every 80 ms; on the other hand, $\mathrm{SID} = (\mathrm{BeamMaxDelay} - \mathrm{Delay})$, which is usually low and therefore we will neglect it in the sequel.

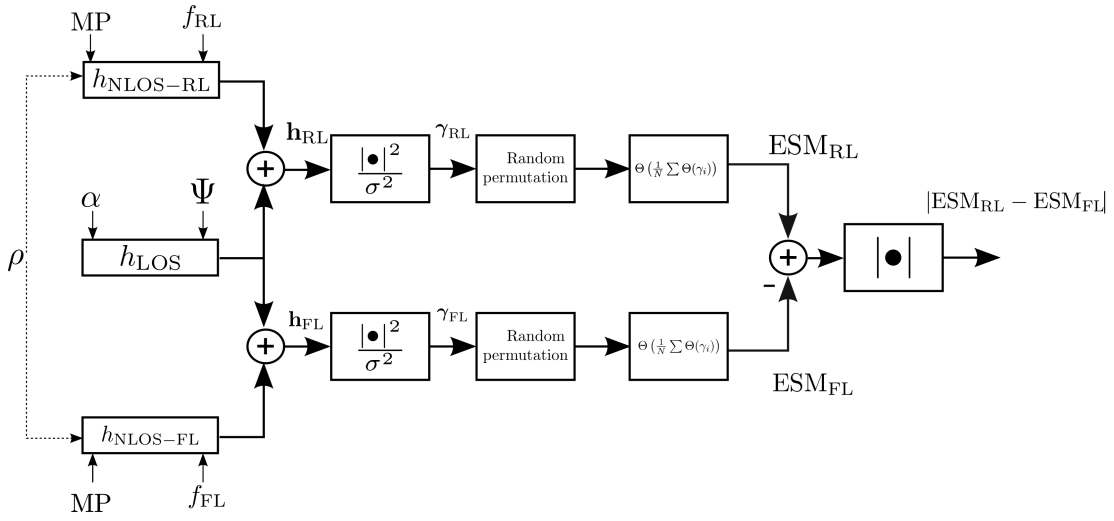

Figure 5. Simulation setup for open-loop CSI validation.

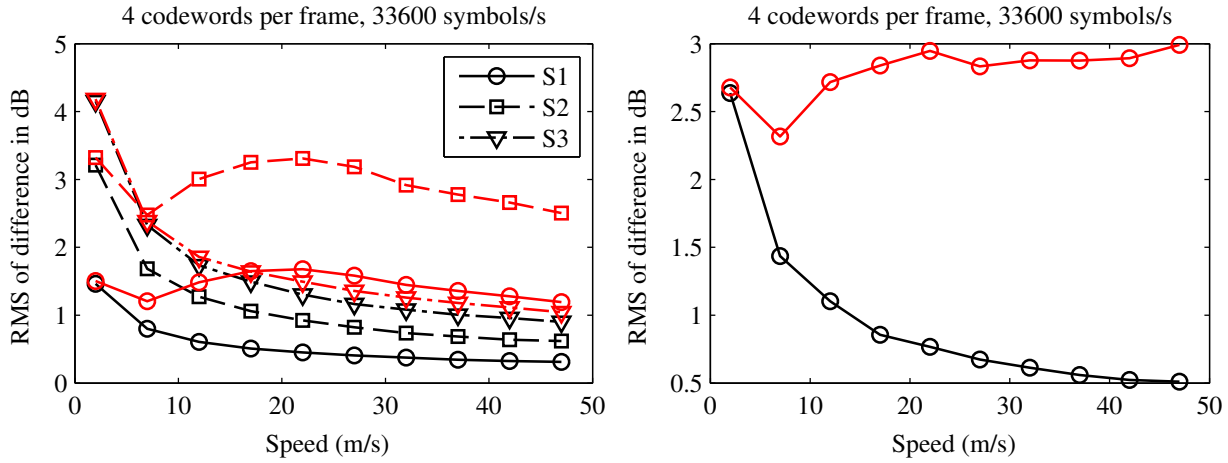

Figure 6. RMS of the ESM difference as a function of speed, $n = 1$, $\mathrm{snr} = 1$; the instantaneous comparison is shown in black, the delayed comparison in red. State by state evolution of the channel on the left, all states together (joint time series) on the right.

B. Simulator description

To test the validity of open-loop CSI, we performed several simulations. The procedure, summarized in Figure 5, is the following:

1) The parameters are $f_{\mathrm{FL}} = 1550\,\mathrm{MHz}$, $f_{\mathrm{FL}} = 1650\,\mathrm{MHz}$ and $T_{\mathrm{symb}} = 1/33600\,\mathrm{s}$.
2) We generate FL and RL channels with the same LOS but uncorrelated NLOS.
3) From the channel samples we obtain a sequence of instantaneous SINR (γ_{FL} and γ_{RL}), and apply interleaving on them.
4) We compute the effective SNR mapping (ESM) as detailed in Section II-B.
5) The ESM values, in dB, are compared, and the absolute value of the difference is the output of the simulator.

Additionally, before comparing the values in dB, we may apply a *shift* in order to account for the $n \cdot 80\,\mathrm{ms}$ delay introduced by the standard.

C. Results

We will now report the most relevant simulation results obtained. We focus on a scheme with four codewords per frame, which means that the codeword duration is $20\,\mathrm{ms}$; at this stage, however, we always perform interleaving on an $80\,\mathrm{ms}$ basis, for simplicity. All the simulations in this section have emulated an Intermediate Tree Shadowed (ITS) area. We will plot the root mean squared error (RMS) of the ESM difference $\mathbf{d}$, defined as $\mathrm{RMS} \doteq \sqrt{\frac{1}{N}\sum_{i=1}^{N} d_i^2}$, as a function of the terminal speed.

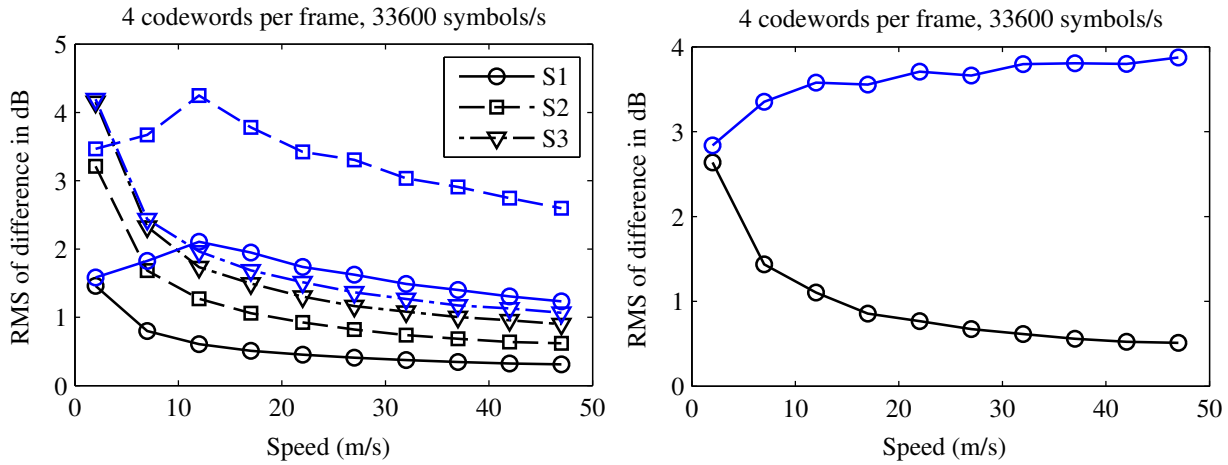

Figure 7. RMS of the ESM difference as a function of speed, $n = 2$, $\mathrm{snr} = 1$. The instantaneous comparison is shown in black, the delayed comparison in blue. State by state evolution of the channel on the left, joint time series on the right.

1) Results with an $80\,ms$ *delay:* Figure 6 shows the comparison result when $n = 1$ –that is, when there is a delay of $80\,\mathrm{ms}$ before transmitting– for $\mathrm{snr} = 1$ ($0\,\mathrm{dB}$). We can see that differences decrease with speed for the instantaneous comparison (black curves), and that they are larger in the states with larger NLOS power. In what refers to the delayed comparison, it is worth noticing the huge differences induced by state 2: they are due to its fast variations in the LOS component, that render a very different channel after waiting for $80\,\mathrm{ms}$.

2) Results with a $160\,ms$ *delay:* Figure 7 shows the comparison result when $n = 2$ –that is, when there is a delay of $160\,\mathrm{ms}$ before transmitting– for $\mathrm{snr} = 1$. The same conclusions as for the previous plot hold; only that, as expected, differences in the delayed case are now larger.

In view of the numerical results, open-loop CSI will be applicable for many speeds, as the most frequent differences are quite low. However, this does not mean that it will outperform traditional closed-loop CSI in each and every case; in particular, note that here we are not taking into account the different interference levels in both links (nor the imperfect estimation of the forward link sample). In the next section, we will illustrate the performance of an ACM link using this kind of open-loop CSI.

IV. Performance of open-loop ACM

In the previous section, we tested the applicability of open-loop CSI, concluding that its accuracy seems to be enough to be applied in practice. We still have to show which performance does it provide in terms of throughput and availability of the link, and whether it brings any advantage over traditional closed-loop CSI or not. In this section, we report the results of the simulations we performed, aimed at comparing a BGAN-type system with one based on open-loop CSI.

A. Simulator description

Even though the suitability test in Section III covered a wide range of cases, here we will focus on a much more specific scenario, as described in Table I. Note that, in assuming a fixed fading bandwidth, we are implicitly assuming that the terminal speed is fixed (and, in this case, equal to $4\,\mathrm{m/s}$). Also, we focused on codewords spanning $20\,\mathrm{ms}$, since this is the most common case for Demand Assigned Multiple Access (DAMA).

Terminal type	Pocket	T_{symb}	$1/16800\,\mathrm{s}$
Environment	ITS	Fading bandwidth	$20\,\mathrm{Hz}$
C/N_0	$50.9\,\mathrm{dBHz}$	f_{FL}	$1550\,\mathrm{MHz}$
Bearer bandwidth	$21\,\mathrm{KHz}$	f_{RL}	$1650\,\mathrm{MHz}$

Table I
Link budget and other parameters used during the simulations.

Figure 8 summarizes the simulation procedure, which we describe in the following items. For each case, we simulated four totally independent channel realizations, with 10^5 codewords in each one.

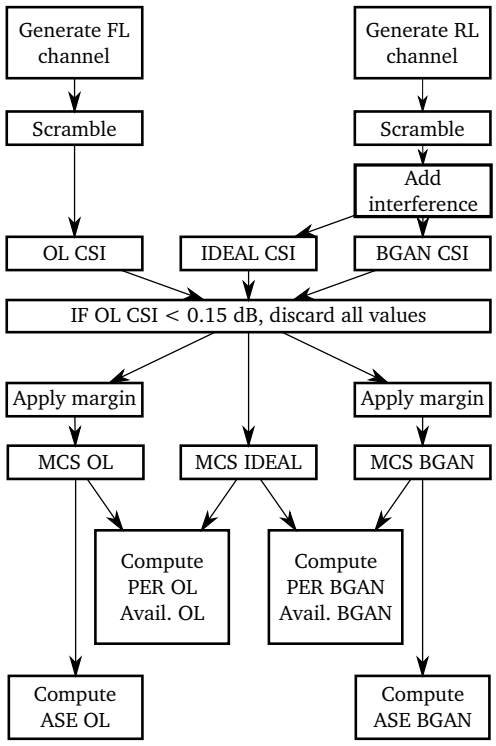

Figure 8. ACM simulation description.

1) Channel generation: We start by generating both channels with the parameters from Table I; this returns the channel coefficients h_k. We compute the SNR as $\mathrm{SNR} = 50.9 - 10\log_{10}(21000) = 7.7\,\mathrm{dB}$, and then use it in natural units, $\mathrm{snr} = 10^{\mathrm{SNR}/10}$.

2) Adding interference: With the above, we would have the sequence of instantaneous SNR, given by $\mathrm{snr}|h_k|^2$. But what we will need for the simulations is actually the sequence of SINR. To obtain it, we used STYLIST and simulated a 62-beam European coverage with the same link budget and parameters as reported above. As an output of the simulation we obtained the sequence of C/I values, which we post-processed to obtain the empirical cumulative distribution function (CDF) of the interference for two different beams, as already shown in Section II-A2. Dragging *one sample per codeword* from the empirical CDF, and using the fact that

$$\left(\frac{C}{N+I}\right)^{-1} = \left(\frac{C}{N}\right)^{-1} + \left(\frac{C}{I}\right)^{-1} \tag{6}$$

we could link both outputs and obtain the SINR values.

3) Computing CSI values: To compare our system with a BGAN-like one, we need to obtain both types of CSI and then select the coding scheme based on it.

- **BGAN CSI:** We obtained it by averaging the instantaneous SINR of the return link (closed-loop) during $0.96\,\mathrm{s}$; we then wait for $0.5\,\mathrm{s}$ (an RTT) before using it.
- **Open-loop CSI:** This is the last ESM sample computed on the forward link signal, with a delay of $80\,\mathrm{ms}$ (since we are assuming $20\,\mathrm{ms}$ codewords).
- **Ideal CSI:** This is the name we give to the *actual, totally accurate* CSI of the channel obtained with no delay.

4) Transmission control protocol: We implement a transmission control policy so that, when the measured quality of the channel is very low, we do nothing. This was done by applying a threshold to the open-loop CSI: if it was below $0.15\,\mathrm{dB}$, the threshold for the most protected coding scheme of the bearer in use, we did not test anything.

5) Transmitted symbols: In this work, we focused on the bearer R20T0.5Q-1B, which uses only QPSK modulation; the coding schemes available for this bearer can be seen on Table II, along with some details on their efficiency.

6) MCS selection: From a given CSI value, the corresponding coding rate is selected by applying a threshold. In this work, thresholds have been selected by tial-and-error to meet a PER constraint of 10^{-3}, using the outputs of Section III as guidance;

	L8	L7	L6	L5	L4	L3	L2	L1	R
γ_{th} (dB)	0.15	0.91	1.87	2.79	3.90	5.07	5.71	6.48	7.67
Coding rate	0.34	0.39	0.46	0.53	0.61	0.69	0.73	0.77	0.81
Info bits	168	200	240	280	328	376	400	424	448

Table II
CODING RATE OPTIONS FOR THE R20T0.5Q-1B BEARER.

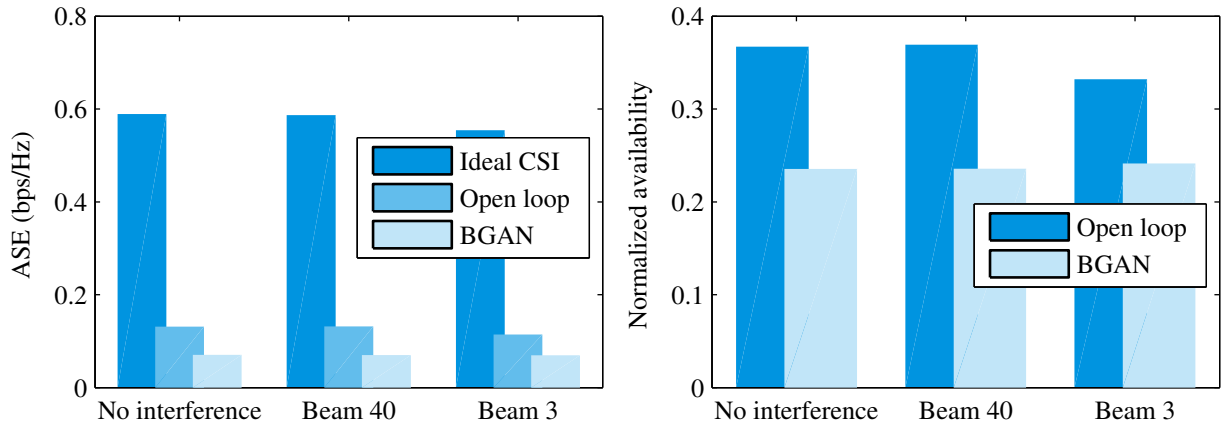

Figure 9. ASE (left) and availability (right) comparison for an ITS environment.

see Table III for the numeric values. If the value obtained after applying the margin is below the threshold of the most protected MCS, we say to select $\text{MCS} = 0$, which means that we do not transmit at all.

	No interference		Beam 40		Beam 3	
	BGAN	Open-loop	BGAN	Open-loop	BGAN	Open-loop
Open	2.15	1.8	2.15	1.9	3.95	4.8
ITS	7.7	6.8	7.6	6.8	6.7	7.1

Table III
MARGINS USED FOR MCS SELECTION, IN DB. OBTAINED BY TRIAL AN ERROR TO ENSURE $\text{PER} = 10^{-3}$.

7) Computation of the results: The results of the simulation are offered in terms of average spectral efficiency (ASE), availability and packet error rate (PER), which we define as follows.

- **ASE:** Average spectral efficiency of the coding rate selected (recall that the modulation is always QPSK).
- **PER:** Let MCS_k^0 be the sequence of coding schemes we would have selected using perfect, ideal CSI of the channel, and let $\mathcal{I}[P]$ be the indicator function, which takes the value 1 when P is true and 0 otherwise; for a sequence of coding schemes $\{\text{MCS}_k\}_{k=1}^K$, we compute the PER as $\text{PER} = \frac{1}{K}\sum_{k=1}^K \mathcal{I}\left[\text{MCS}_k > \text{MCS}_k^0\right]$
- **Availability:** We consider that a link is available whenever the selected MCS is different from zero, that is $\text{Availability} = \frac{1}{K}\sum_{k=1}^K \mathcal{I}[\text{MCS} > 0]$. Also, we call it *normalized availability* when it is normalized by the availability obtained with ideal CSI, which is the maximum performance we could obtain.

B. Performance results

Here, we will present the results obtained for two different environments: ITS and open. Using three different interference profiles, we will illustrate the potential of open-loop adaptation. Although the target scenario is ITS, we simulated the other one in order to test how well does the designed system perform in other conditions.

1) Best performance: ITS: Figure 9 depicts a comparison in terms of ASE and availability between the two techniques considered for an ITS environment. The gain in performance is remarkable: **close to** 92 **% in terms of ASE, and** 12 **% more availability** even for the most compelling interference pattern (beam 3).

Note that these gains come with no loss in terms of PER: Figure 10 proves this fact, showing that a BGAN-like system can be allowed a slightly higher PER without reaching the same ASE as the open-loop alternative.

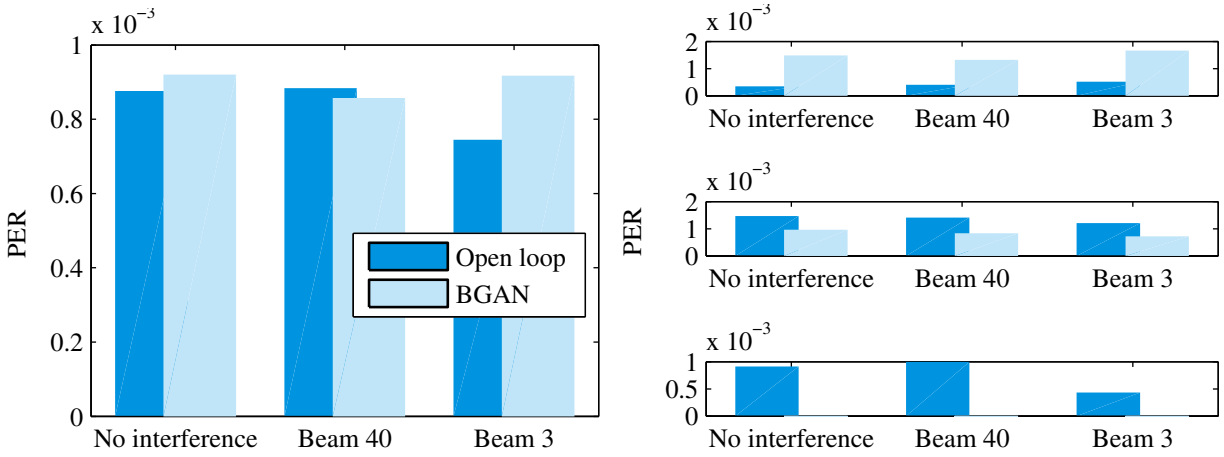

Figure 10. PER (left) and state-by-state PER (right) comparison for an ITS environment.

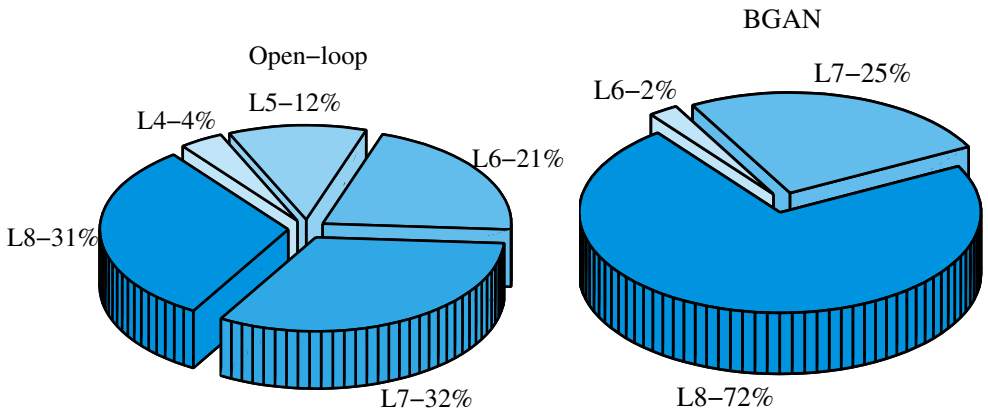

Figure 11. Percentage of usage of each MCS for open-loop (left) and BGAN (right), ITS environment, beam 3.

For a better understanding of the results, Figure 11 shows the percentage of usage of each coding scheme with the strongest interference distribution. We can see that, while BGAN uses the most protected mode 72 % of the time, an open-loop strategy explores up to L4 without losing in terms of PER.

2) Intermediate performance: open environment: Figures 12,13 show the same results as above, but now for an open environment. As we can see, performance gains here are much smaller, if any. In fact, with the higher interference levels that beam 30 provides, open-loop performs slightly below BGAN.

The explanation in this case is easy: an open environment is easy to track, even using average SNR and affording long delays. On the other hand, open-loop is unaware of the interference level, which must be counteracted by enlarging the MCS selection margins. As a result, there is no advantage in using it, and it can even perform worse.

Finally, Figure 14 shows the MCS distribution, again for the case with the strongest interference.

V. Conclusions

In this work, we have tested the applicability of open-loop ACM in the return link of a mobile satellite link using, for improved performance monitoring, effective SNR metrics instead of conventional average SINR as CSI.

After a careful study of the two CSI alternatives, we carried out a performance test focusing on specific working conditions. We used the simplest way to exploit the obtained CSI: the last CSI sample is used, after applying a margin, to select the most suitable MCS by comparing this value with its working threshold.

As summarized on Table IV, results have shown that, for the scenario under study, the best performance is obtained in an ITS environment, reaching up to 92 **% in terms of ASE, and** 12 **% more availability**, even for the most compelling return link interference pattern simulated.

Open-loop adaptation outperforms conventional techniques because the obtained CSI is up to date, and in many cases also more accurate. However, in a slowly varying channel with large interference (which we are accounting for by a fixed margin),

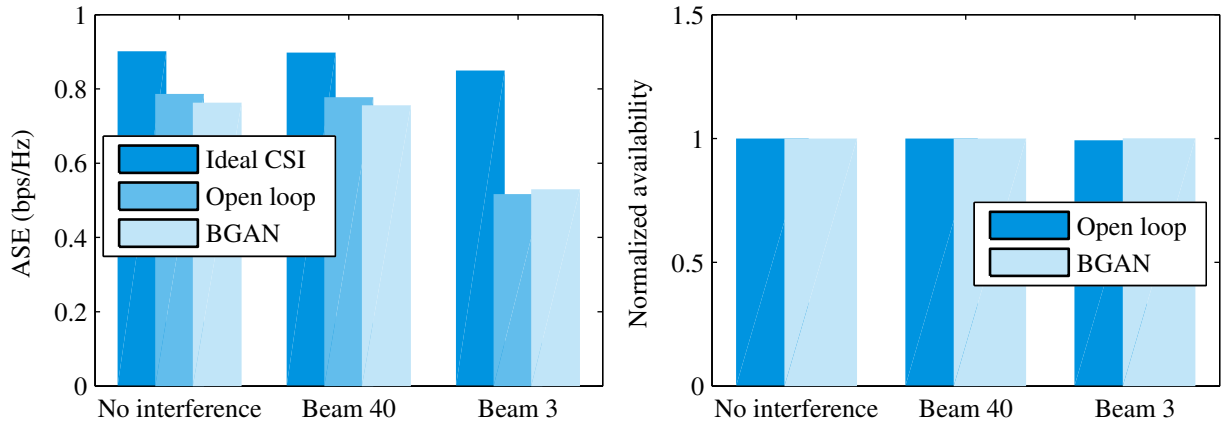

Figure 12. ASE (left) and availability (right) comparison for an open environment.

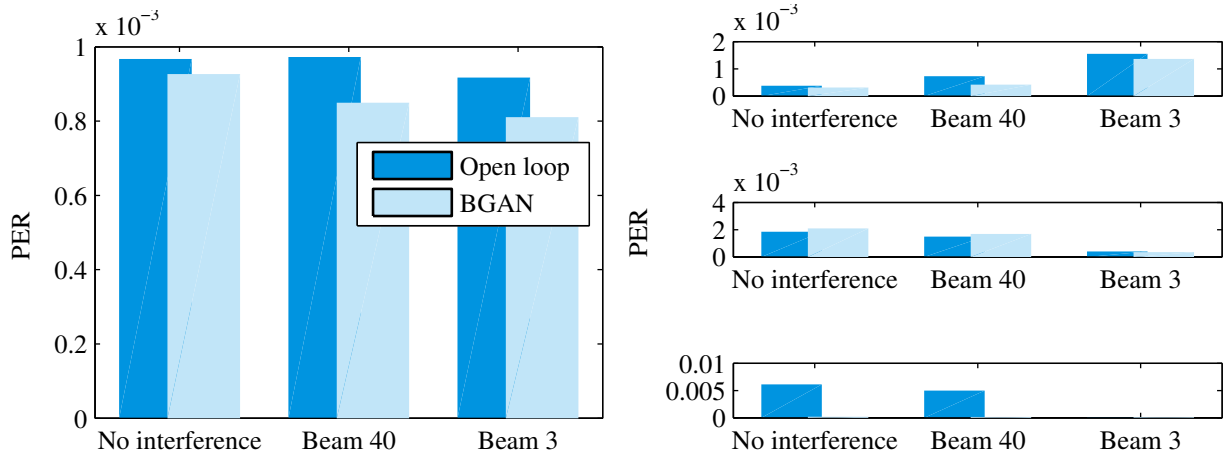

Figure 13. PER (left) and state-by-state PER (right) comparison for an open environment.

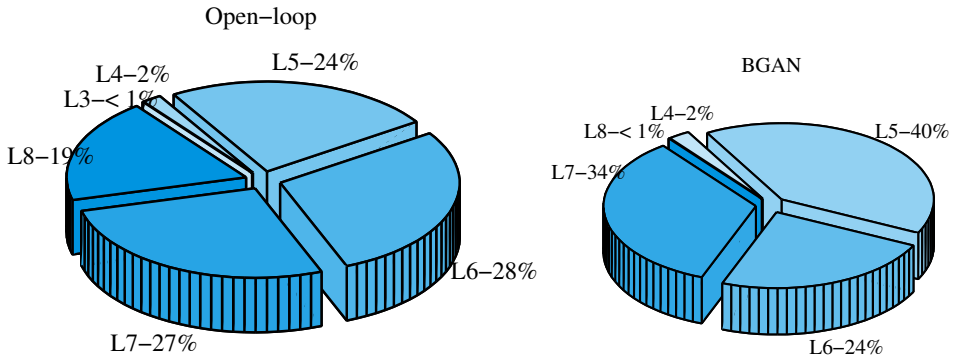

Figure 14. Percentage of usage of each MCS for open-loop (left) and BGAN (right), open environment, beam 3.

	No interference		Beam 40		Beam 3	
	BGAN	Open-loop	BGAN	Open-loop	BGAN	Open-loop
Open	0.7627	0.7862	0.7558	0.7776	0.5298	0.5166
ITS	0.0702	0.1314	0.0701	0.1319	0.0694	0.1141

Table IV
SUMMARY OF THE ASE (BPS/HZ) RESULTS OBTAINED.

conventional closed-loop techniques could potentially be more effective. As a further line of research, we propose to use more samples of the measured ESM[3] jointly with a better characterization of interference, which could allow a better use of the channel.

VI. ACKNOWLEDGEMENTS

Work supported by the European Space Agency under project "Adaptive Transmission Techniques for Mobile SatCom", purchase order No. 5401001280, and by the European Regional Development Fund (ERDF) and the Spanish Government under project DYNACS (TEC2010-21245-C02-02/TCM).

The authors would like to thank P. Daniel Arapoglou, Alberto Ginesi, Riccardo de Gaudenzi and Martina Angelone for their advice and support during the project.

REFERENCES

[1] H. Bischl, H. Brandt, T. de Cola, R. De Gaudenzi, E. Eberlein, N. Girault, E. Alberty, S. Lipp, R. Rinaldo, B. Rislow, J. A. Skard, J. Tousch, and G. Ulbricht, "Adaptive coding and modulation for satellite broadband networks: From theory to practice," *International Journal of Satellite Communications and Networking*, vol. 28, no. 2, pp. 59–111, 2010. [Online]. Available: http://dx.doi.org/10.1002/sat.932

[2] F. Perez Fontan, M. Vazquez Castro, C. Enjamio Cabado, J. Pita Garcia, and E. Kubista, "Statistical modeling of the LMS channel," *IEEE Trans. Vehicular Technology*, vol. 50, pp. 1549–1567, Nov. 2001.

[3] J. Arnau, A. Rico-Alvariño, and C. Mosquera, "Adaptive transmission techniques for mobile satellite links," in *30th AIAA International Communications Satellite Systems Conference (ICSSC)*, Ottawa, Canada, 2012.

[4] ETSI TS 102 744, "Satellite Component of UMTS (S-UMTS); Family SL satellite radio interface," Oct. 2012, draft.

[5] C. Loo, "A statistical model for a land mobile satellite link," *IEEE Trans. Vehicular Technology*, vol. 34, pp. 122–127, Aug. 1985.

[6] F. Gini, M. Luise, and R. Reggiannini, "Cramer-Rao bounds in the parametric estimation of fading radiotransmission channels," *IEEE Trans. Commun.*, vol. 46, pp. 1390–1398, Oct. 1998.

[7] P. Burzigotti, R. Prieto-Cerdeira, A. Bolea-Alamanac, F. Perez-Fontan, and I. Sanchez-Lago, "DVB-SH Analysis Using a Multi-State Land Mobile Satellite Channel Model," in *Advanced Satellite Mobile Systems, 2008. ASMS 2008. 4th*, aug. 2008, pp. 149 –155.

[8] SpE, "STYLIST: SW Tool for HYbrid SateLlite / TerrestrIal mobile BroadcaSting SysTem," available at http://telecom.esa.int/telecom/www/object/index.cfm?fobjectid=32112.

[9] R. G. Gallager, *Information Theory and Reliable Communication*. New York, NY, USA: John Wiley & Sons, Inc., 1968.

[10] "216715 newcom++ dr.3.3 final report: Amc design towards next generation wireless systems."